Received: 9 April 2023 | Accepted: 4 September 2023

DOI: 10.1002/vzj2.20283

Vadose Zone Journal

ORIGINAL ARTICLE

A numerical test of soil layering effects on theoretical and practical Beerkan infiltration runs

Vincenzo Bagarello[1,2] | **Massimo Iovino**[1] | **Jianbin Lai**[3]

[1]Department of Agricultural, Food and Forest Sciences, University of Palermo, Palermo, Italy

[2]Centro Interdipartimentale di Ricerca "MIGRARE. Mobilità, differenze, dialogo, diritti", University of Palermo, Palermo, Italy

[3]Yucheng Comprehensive Experimental Station, Institute of Geographic Sciences and Natural Resources Research, Chinese Academy of Sciences, Beijing, China

Correspondence
Jianbin Lai, Yucheng Comprehensive Experimental Station, Institute of Geographic Sciences and Natural Resources Research, Chinese Academy of Sciences, Beijing 100101, China. Email: laijianbin@igsnrr.ac.cn

Assigned to Associate Editor Behzad Ghanbarian.

Funding information
European Union Next-GenerationEU (National Recovery and Resilience Plan), Grant/Award Numbers: D.D. 1243 2/8/2022, PE0000005; National Natural Science Foundation of China, Grant/Award Number: U22A20555

Abstract

With reference to a more compacted and less conductive upper soil layer overlying a less compacted and more conductive subsoil, a simple three-dimensional (3D) infiltration run is expected to yield more representative results of the upper layer than the subsoil. However, there is the need to quantitatively establish what is meant by more representativeness. At this aim, numerically simulated infiltration was investigated for a theoretically unconfined process under a null ponded head of water (d0H0 setup, with d = depth of ring insertion and H = ponded depth of water) and a practical Beerkan run (d1H1 setup, $d = H = 1$ cm). The considered layered soils differed by both the layering degree (from weak to strong; subsoil more conductive than the upper soil layer by 2.3–32.4 times, depending on the layering degree) and the thickness of the upper soil layer (0.5–3 cm). It was confirmed that water infiltration should be expected to be more representative of the upper soil layer when this layer is the less permeable since, for a 2-h experiment, the instantaneous infiltration rates for the layered soil were 1.0–2.1 times greater than those of the homogeneous low-permeable soil and 1.3–20.7 smaller than those of the homogeneous coarser soil that constituted the subsoil. Similarity with the homogeneous fine soil increased as expected as the upper layer became thicker. For a weak layering condition, the layered soil yielded an intermediate infiltration as compared with that of the two homogeneous soils forming the layered system. For a strong layering degree, the layered soil was more similar to the homogeneous fine soil than to the homogeneous coarse soil. Using the practical setup instead of the theoretical one should have a small to moderate effect on the instantaneous infiltration rates since all the calculated percentage differences between the d1H1 and d0H0 setups fell into the relatively narrow range of −18.8% to +17.4%. A sequential analysis procedure appeared usable to detect layering conditions but with some modifications as compared with the originally proposed procedure. The practical setup enhanced the possibility to recognize the time at which the characteristics of the subsoil start to influence the infiltration process. In conclusion, this investigation contributed to better interpret both the theoretical and the practically established 3D infiltration process in a soil composed of a less

conductive upper soil layer overlying a more conductive subsoil and it also demonstrated that modifying the recently proposed sequential analysis procedure only using infiltration data could be advisable to determine the time when layering starts to influence the process.

1 | INTRODUCTION

Soil hydraulic properties are frequently estimated by establishing a three-dimensional (3D) infiltration process through a circular source into the initially unsaturated soil. Such a kind of infiltration process depends on gravity and on both vertical and lateral capillarity (Vandervaere et al., 2000). The applied experimental methodology and the time window to which the data refer can differ from case to case. In particular, the experiment can be carried out by establishing a ponded head of water or a negative pressure head on the infiltration surface. Both the transient and the steady-state stages of the process can be sampled but the data could also be collected for only one of the two stages. Regardless of these differences, the vast majority of data analysis methods rely on 3D infiltration models that were developed under the assumption that the data are representative of an ideal soil, that is, homogeneous, isotropic, rigid, and uniformly unsaturated at the beginning of the experiment (Angulo-Jaramillo et al., 2016). However, ideal soil conditions are rarely, if ever, met in the field and efforts must be made to find a link between theory and reality.

Infiltration experiments can be carried out, sometimes with no or little awareness, on soil volumes that consist of two layers with different hydraulic properties. In particular, a compacted soil layer, more or less thin, overlying a less compacted subsoil is rather common in different environments and conditions and its presence can have a large impact on hydrological processes, soil-water relations, and soil physical quality (Assouline & Mualem, 2002; Ben-Hur et al., 1987; Lenhard, 1986; Ramos et al., 2000; Reynolds et al., 2009). A less permeable upper layer can be formed as a consequence of soil sealing (Assouline & Mualem, 1997), compaction (Assouline et al., 1997), settlement of sediments in urban infiltration basins (Lassabatere et al., 2010), or in engineered soils (Yilmaz et al., 2013). The thickness of this upper layer can vary widely, depending on the circumstances. For example, Assouline (2004) and Moret-Fernández et al. (2021) reported values of seal thickness varying from <1 to 20 mm and from 10 to 50 mm, respectively. Batey (2009) stated that, at least in particular situations, the compaction depth may extend to 1 m or more.

The number of documents examining 3D infiltration processes into layered soils seems to be limited (Dohnal et al., 2016; Shan & Stephens, 1995; Wu et al., 1997), but some studies specifically considered the case of a low-permeable layer over a more permeable layer. In particular, Lassabatere et al. (2010) and da Silva Ribas et al. (2021) suggested that, when the soil is layered and the upper layer is the less permeable, water infiltration is more representative of the upper layer. A similar result was obtained by Yilmaz et al. (2013), sampling temporal changes of a basic oxygen furnace slag. Di Prima et al. (2018) tested in the laboratory infiltration in a sealed soil and they recognized that the process was mainly governed by seal formation and also that the final infiltration rates were representative of the hydraulic behavior of the seal layer, irrespective of the upper soil layer thickness. Working in the field in a Mediterranean vineyard, Alagna et al. (2019) also suggested that a simple infiltration experiment is suitable enough to detect the effect of the altered upper layer on flow. Recently, Moret-Fernández et al. (2021) developed a method to analyze the 3D infiltration data collected in layered soils regardless of whether the upper soil layer is finer or coarser than the subsoil. In particular, the time when the infiltration bulb reaches the interface between the upper soil layer and the subsoil can be identified by sequentially fitting a cumulative infiltration model to the data and then examining how the root mean square error, RMSE, changes during the run. This is consistent with the fact that some of the properties of the deeper soil layer can be expected to influence the measured infiltration. In the absence of any soil layering, RMSE should remain nearly constant while it suddenly increases when the infiltration bulb reaches the interface of layers in layered soils. Moret-Fernández et al. (2021) obtained encouraging results by applying the sequential analysis procedure with the four-term approximation of the cumulative infiltration model by Haverkamp et al. (1994), as proposed by Moret-Fernández et al. (2020).

Therefore, with reference to a more compacted and less conductive upper layer overlying a less compacted and more conductive subsoil, the expectation is that a simple 3D infiltration run will yield more representative results for the upper layer than the subsoil (da Silva Ribas et al., 2021; Lassabatere et al., 2010) and that the measured infiltration will contain (Moret-Fernández et al., 2021), but not necessarily in a perceivable manner (Di Prima et al., 2018), some information related to the subsoil. These conclusions require further investigations to better establish what is meant in practice when one speaks of an infiltration curve being more representative of the upper layer and also what factors influence this similarity and how.

BEST (Beerkan Estimation of Soil Transfer parameters) methods of 3D infiltration data analysis (Bagarello et al., 2014; Lassabatere et al., 2006; Yilmaz et al., 2010) are largely used to obtain a complete soil hydraulic characterization (Angulo-Jaramillo et al., 2019). They are based on the theoretical description of the infiltration process with the Haverkamp et al. (1994) model that was specifically developed to analyze a fully 3D process under a pressure head not greater than zero. Therefore, the use of this model to deduce the saturated soil hydrodynamic parameters is theoretically limited to the case of a ring insertion depth, d, equal to zero and also a null ponded depth of water on the infiltration surface ($H = 0$). Establishing an unconfined 3D infiltration process under a null ponded depth of water is not easy from an experimental point of view. In particular, it may require performing a relatively complicated experiment with the tension infiltrometer, which is not free from uncertainties and problems such as those concerning the hydraulic contact between the device and the soil surface (Close et al., 1998). More easily, a Beerkan infiltration run could be performed since literature suggests that it should be representative of such a kind of infiltration process (Lassabatere et al., 2006). A Beerkan run is performed by inserting a small ring (with a radius of ≤100 mm) in the soil to a short depth (∼10 mm) to avoid lateral loss of water and then by establishing an infiltration process under a near null ponded depth of water. In the simplest cases, small (≤140 mL) and constant water volumes are poured repeatedly on the soil surface until the process stabilizes (Lassabatere et al., 2006). However, the experimental data obtained by this type of run agree only approximately with the theoretical assumptions of the infiltration model by Haverkamp et al. (1994) since inserting the ring into the soil implies that infiltration is forced to be one-dimensional (1D) at the beginning of the run. In addition, repeatedly pouring a small water volume into the ring or using automated infiltrometers (Di Prima, 2015) determine a small positive pressure head on the soil surface for at least a part of the experiment. For example, in the paper by Lassabatere et al. (2006), the initial ponded depth of water was of 0.2–0.8 cm, depending on the run. An initial ponded depth of water of 1.1 cm was reported by Xu et al. (2012).

With reference to five ideal soils, Bagarello et al. (2022) recently established a numerical comparison between the theoretical ($d = H = 0$) and the practical ($d = H = 1$ cm) setups. A constant H value of ∼1 cm can be considered as a rather extreme case for a Beerkan infiltration run. Therefore, the term practical setup was used to denote an experimental setup similar but not identical to the theoretical setup assuring a perfect consistency between the infiltration model (Haverkamp et al., 1994) and the experiment. Inserting the ring a little into the soil reduced the instantaneous infiltration rates, i_r, for the entire run and hence cumulative infiltration, I, while establishing a small ponded depth of water on the infiltration surface increased i_r and I. Generally, the two effects, even if they had an opposite sign, did not compensate one with other without a residual. In any case, differences between the two setups, denoted as d0H0 and d1H1 for the theoretical and practical situations, respectively, were small and perhaps negligible in many practical circumstances since they did not exceed a few percentage units (∼10%) for both i_r and I.

Testing setup effects on layered soils is necessary to verify if this conclusion also applies to a more complex scenario. In the case of a layered soil, it can be presumed that, depending on the thickness of the upper layer relative to the ring insertion depth, infiltration into this layer will exclusively be 1D or 3D after a 1D phase. Similarly, infiltration in the subsoil can exclusively be 3D or 3D after a 1D phase.

Numerical simulation appears an appropriate tool for testing layering and setup effects on the infiltration process since a numerical experiment makes it possible to determine how a specific factor influences the soil hydrodynamic response and it can be performed in fully controlled conditions, without any experimental error (e.g., Bagarello et al., 2019, 2022; Dohnal et al., 2016; Lai & Ren, 2007; Lai et al., 2010; Reynolds, 2013; Wu et al., 1993).

The general objective of this investigation was to verify the impact of a low-permeable soil layer overlying a more permeable subsoil on a theoretically unconfined process under a null ponded depth of water (d0H0 setup) as well as a practical Beerkan run (d1H1 setup). The specific objectives were to (i) determine the impact of the soil layering degree and the thickness of the upper layer on infiltration rates and cumulative infiltration; (ii) test the applicability of the recently suggested sequential analysis procedure to identify the time when the infiltration front reaches the subsoil; and (iii) verifying if and in what situations a theoretical analysis that assumes a fully unconfined process under a null ponded depth of water can be considered appropriate for a Beerkan infiltration run performed on a layered soil.

Core Ideas

- Beerkan infiltration in layered soil was numerically studied for both theoretical setup and practical approximation.
- Using the practical setup instead of the theoretical one should have small to moderate effect on infiltration rates.
- Modified sequential analysis procedure is usable to detect layering conditions in practical infiltration.

TABLE 1 Soil hydraulic parameters (Carsel & Parrish, 1988) and initial soil water content for the numerical simulations.

	van Genuchten–Mualem parameters					
Soil	θ_r (cm^3/cm^3)	θ_s (cm^3/cm^3)	α (1/cm)	n	K_s (cm/s)	θ_i (cm^3/cm^3)
Loamy-sand, LS	0.057	0.41	0.124	2.28	4.05×10^{-3}	0.057
Sandy-loam, SAL	0.065	0.41	0.075	1.89	1.23×10^{-3}	0.066
Loam, L	0.078	0.43	0.036	1.56	2.88×10^{-4}	0.092
Silt-loam, SIL	0.067	0.45	0.020	1.41	1.25×10^{-4}	0.113

Note: θ_r, residual volumetric soil water content; θ_s, saturated volumetric soil water content; α and n, empirical parameters of the van Genuchten (1980) model for the water retention curve; K_s, saturated soil hydraulic conductivity; θ_i, initial volumetric soil water content.

TABLE 2 The practical and theoretical Beerkan infiltration scenarios under nine combinations of layered soil.

Layered soil	**Practical Beerkan run (d1H1)**			**Theoretical Beerkan run (d0H0)**		
Upper soil	**Silt-loam**			**Silt-loam**		
Lower soil	**Loam**	**Sandy-loam**	**Loamy-sand**	**Loam**	**Sandy-loam**	**Loamy-sand**
	Layering degree					
Upper layer thickness (cm)	**Weak**	**Moderate**	**Strong**	**Weak**	**Moderate**	**Strong**
0.5	SIL0.5L	SIL0.5SAL	SIL0.5LS	SIL0.5L	SIL0.5SAL	SIL0.5LS
1	SIL1L	SIL1SAL	SIL1LS	SIL1L	SIL1SAL	SIL1LS
3	SIL3L	SIL3SAL	SIL3LS	SIL3L	SIL3SAL	SIL3LS

Abbreviations: L, loam; LS, loamy-sand; SIL, silt-loam; SAL, sandy-loam.

2 | MATERIALS AND METHODS

2.1 | Soils and numerical experiments

Four soils, namely silt-loam (SIL), loam (L), sandy-loam (SAL), and loamy-sand (LS), were considered in this study. Soil hydraulic properties were expressed according to the van Genuchten–Mualem model (Mualem, 1976; van Genuchten, 1980) with hydraulic parameters adopted from Carsel and Parrish (1988) (Table 1). Infiltration experiments were numerically simulated using Hydrus-2D/3D (Šimůnek et al., 2007), which was found to be a robust and reliable tool for simulating water flow in the soil under various conditions (Šimůnek et al., 2016; Varvaris et al., 2021).

Simulations were carried out for the four homogeneous soils (SIL, L, SAL, and LS) as well as nine layered soils as follows: SIL (thickness = 0.5 cm) on L (being denoted as SIL0.5L), SIL (thickness = 1 cm) on L (SIL1L), SIL (thickness = 3 cm) on L (SIL3L), SIL (thickness = 0.5 cm) on SAL (SIL0.5SAL), SIL (thickness = 1 cm) on SAL (SIL1SAL), SIL (thickness = 3 cm) on SAL (SIL3SAL), SIL (thickness = 0.5 cm) on LS (SIL0.5LS), SIL (thickness = 1 cm) on LS (SIL1LS), and SIL (thickness = 3 cm) on LS (SIL3LS) (Table 2). Therefore, three layering degrees were considered in this investigation, namely, a weakly layered soil (SIL over L; $K_{lo}/K_{up} = K_s$ of the lower layer/K_s of the upper layer = 2.3), a moderately layered soil (SIL over SAL; $K_{lo}/K_{up} = 9.8$), and a strongly layered soil (SIL over LS; $K_{lo}/K_{up} = 32.4$). For each layering degree, three thickness values of the upper soil layer, t_{ul}, were considered.

All simulations were performed with both the d0H0 (null depth of ring insertion, d, and null pressure head on the soil surface, H) and d1H1 ($d = H = 1$ cm) setups. The ring radius was equal to 5 cm and the initial condition was that of a uniform soil water pressure head, $h_i = -9022$ cm. Only this initially dry condition was considered for a threefold reason: (i) the drier the soil the greater the lateral capillarity term, which represents the distinguishing term between 3D and 1D infiltration (Vandervaere et al., 2000); (ii) determining soil hydrodynamic properties with a Beerkan run and the Haverkamp et al. (1994) model requires that the experiment is performed in an initially relatively dry soil (in particular, antecedent soil water content, θ_i, not greater than 0.25 times the saturated soil water content, θ_s, according to Lassabatere et al., 2006); and (iii) with reference to several homogeneous soils, including those considered in this investigation, and a range of relatively small initial soil water content values, differences between the infiltration rates for the d0H0 and d1H1 setups were not appreciably affected by the antecedent soil water content (Bagarello et al., 2022). Defining the initial conditions with a constant soil water pressure head in the entire flow domain finds support in the literature (Dohnal et al., 2016; Dušek et al., 2009). In particular, these authors simulated 3D infiltration processes in an initially dry soil by fixing h_i at −1000 cm. However, with this h_i value, the θ_i/θ_s ratio was equal to 0.29 for the L soil and 0.40 for the SIL

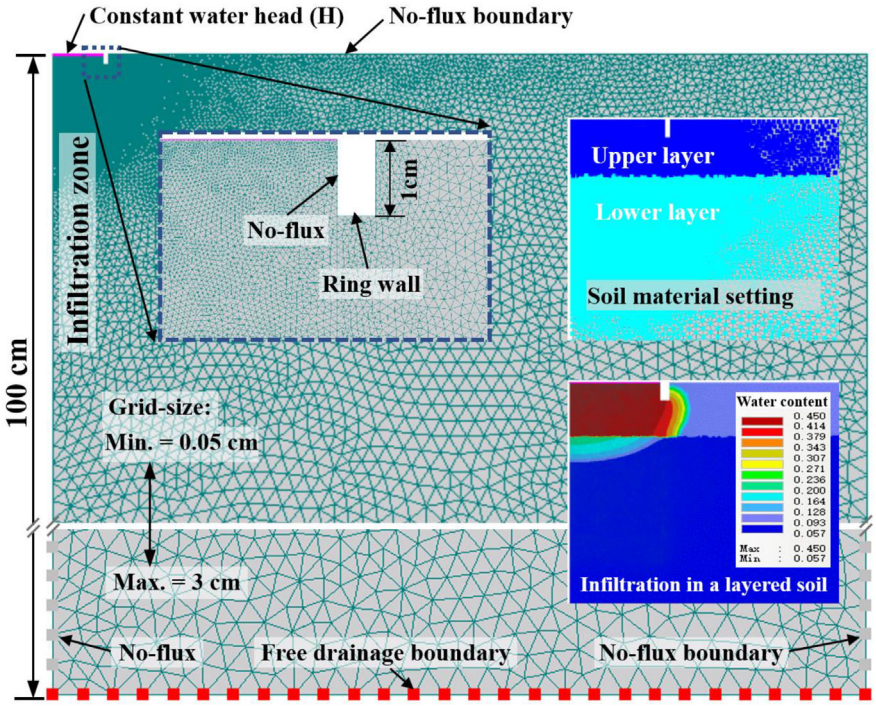

FIGURE 1 Schematic of the flow domain and settings for the numerical simulations.

soil and hence it was incompatible with the possible application of BEST methods of analysis of 3D infiltration data (Lassabatere et al., 2006). A smaller h_i value (−9022 cm) was therefore considered in this investigation. In this case, θ_i/θ_s did not exceed 0.25 for the four tested soils. Each infiltration process was simulated for 2 h, in accordance with Dušek et al. (2009), and also considering that this duration likely represents a plausible time limit for a field run in many circumstances. Instantaneous infiltration rate, i_r (L/T), and cumulative infiltration, I (L), data were stored at 12 s time intervals. Infiltration rate was expressive of the process at any particular instant whereas cumulative infiltration integrated infiltration rates until a given instant.

To guarantee an unrestricted flow, the size of the flow domain was 80 cm in X and 100 cm in Z for the L and SIL soils while it was 100 cm in X and 200 cm in Z for the LS and SAL soils (Figure 1). The element size was 0.05 cm for the upper 10 cm of the flow domain and then it gradually increased to a maximum of 3 cm at the bottom. A variable density of element mesh was chosen to ensure the simulation accuracy for a relatively large flow domain. The boundary condition at the bottom was free drainage and no lateral flux was considered for the vertical boundaries of the simulation domain. An upper boundary condition of constant water head was assigned within the ring to simulate infiltration under ponding conditions. Flow was not affected by the established boundaries of the domain during the simulation period. Therefore, the setting of the simulation domain was appropriate to represent the actual infiltration process under the various considered setups. The same methodology of numerical simulation of 3D infiltration experiments was also applied recently by Moret-Fernández et al. (2021).

2.2 | Data analysis

Initially, the data obtained with the d0H0 setup were analyzed according to the following three steps: (i) analysis of the infiltration rates; (ii) analysis of cumulative infiltration; and (iii) testing the sequential analysis procedure by Moret-Fernández et al. (2021).

Concerning the first step, the i_r values of the finest (SIL) homogeneous soil were first compared with those of the homogeneous coarser (L, SAL, and LS) soils. Then, the i_r values obtained for each combination between layering degree (weak, moderate, and strong) and t_{ul} value (0.5, 1, and 3 cm) were compared with those of the two homogeneous soils that were combined with each other to form the layered soil. To define in more detail the link between infiltration in a homogeneous fine soil and infiltration in a layered soil composed of an upper layer of the same fine soil and a coarser subsoil, the infiltration rate ratio, $i_{rLH} = i_r(\text{layered soil})/i_r(\text{SIL})$ (L = layered; H = homogeneous), versus time curves were then examined for the nine layering scenarios.

With reference to the second step of the analysis, focused on cumulative infiltration, it was preliminarily decided to consider the first 0.5 h of the process. This choice was made for a twofold reason: (i) a relatively short infiltration run, allowing to save time and water in intensive field campaigns, has more practical interest than a long run; and (ii) with this duration, it was possible to consider different scenarios, ranging from a process that was presumably affected by layering very soon ($t_{ul} = 0.5$ cm) to a process that occurred in the upper soil layer for an appreciable part of its total duration ($t_{ul} = 3$ cm). The cumulative infiltration curves for the layered and the two corresponding homogeneous soils were compared. The

percent differences between cumulative infiltration of the layered ($I_{layered}$) and the homogeneous SIL (I_{SIL}) soils, $\Delta I_{LH} = 100 \times (I_{layered} - I_{SIL})/I_{SIL}$, were then calculated at each time point during the run.

Concerning the third step of the analysis for the theoretical setup, the methodology by Moret-Fernández et al. (2021) was preliminarily applied by using the four-term approximation of the model by Haverkamp et al. (1994) and (Moret-Fernández et al., 2020) and the "Solver" program built into Microsoft Excel. However, the results were not satisfactory due to the difficulty to obtain valid, that is, non-null, values of the last two coefficients of the model. Perhaps, the used tool or the time interval between two subsequent data points was not appropriate to perform this analysis. Instead, positive, and hence valid, parameters were obtained by considering the infiltration rates instead of cumulative infiltration and fitting the empirical three-term infiltration model by Horton (1940) to the data. Therefore, this last approach was used to verify if the sequential analysis procedure was usable to reveal layering conditions. The use of Horton-type models for the analysis of the 3D infiltration process is already well documented in the scientific literature (Hussen & Warrick, 1993; Iovino et al., 2021; Jacques et al., 2002).

A comparison between the d0H0 and d1H1 setups was subsequently carried out. In particular, the relationship between $\Delta i_{rPT} = 100 \times [i_r(\text{d1H1}) - i_r(\text{d0H0})]/i_r(\text{d0H0})$ (P = practical; T = theoretical) and t was determined for the nine layered soils and also for the homogeneous SIL soil for comparative purposes. Similar calculations were made for cumulative infiltration. In this last case, the relationship between $\Delta I_{PT} = 100 \times [I(\text{d1H1}) - I(\text{d0H0})]/I(\text{d0H0})$ and t was determined. Finally, the effect of the used setup on the results of the sequential analysis procedure was evaluated.

The analysis of the instantaneous infiltration rates was initially performed by considering the simulated data at $\Delta t = 0.2$ min, representing the shortest available time interval. However, in the development of the analysis, it was considered that the cumulative infiltration data, the fitting of a model to the data, and the experimental information collected with the d1H1 setup mainly have a practical relevance since the data collected in the field are frequently used to estimate soil hydrodynamic properties. In this case, it is unlikely that infiltration will be measured at very short time intervals, except for limited time periods. Therefore, the cumulative infiltration data and those obtained with the d1H1 setup were analyzed by considering a longer time interval between two subsequent readings, that is, $\Delta t = 1$ min. The same choice was made to fit an infiltration model to the data.

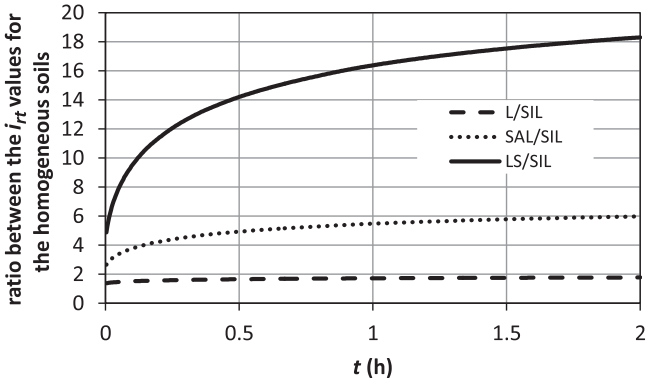

FIGURE 2 Ratio between the infiltration rates, i_r, for the L (loam), SAL (sandy-loam), and LS (loamy-sand) homogeneous soils and those for the homogeneous SIL (silt-loam) soil plotted against time, t.

3 | RESULTS AND DISCUSSION

3.1 | Unconfined infiltration under a null ponded depth of water (d0H0 setup)

3.1.1 | Infiltration rates

As expected, the infiltration rate at any given instant during the 2-h run increased from the less to the most conductive homogeneous soil, that is, according to the LS > SAL > L > SIL order. On average, the $i_r(\text{L})/i_r(\text{SIL})$, $i_r(\text{SAL})/i_r(\text{SIL})$, and $i_r(\text{LS})/i_r(\text{SIL})$ ratios were equal to 1.7, 5.3, and 15.5, respectively (means of 600 values for each ratio), and they increased during the run (Figure 2). In particular, $i_r(\text{L})/i_r(\text{SIL})$ increased by 1.3 times (from 1.4 at $t = 0.2$ min to 1.8 at $t = 2$ h), $i_r(\text{SAL})/i_r(\text{SIL})$ increased by 2.2 times (2.7–6.0) and $i_r(\text{LS})/i_r(\text{SIL})$ increased by 3.7 times (4.9–18.3). Therefore, comparing more similar soils implied obtaining, as expected, infiltration rate ratios that were closer to one and more stable during the run. The $i_r(\text{L})/i_r(\text{SIL})$, $i_r(\text{SAL})/i_r(\text{SIL})$, and $i_r(\text{LS})/i_r(\text{SIL})$ versus t relationships were concave downwards, indicating that the i_r ratios increased at a decreasing rate as t increased and also suggesting that they tended to stabilize at long times, in accordance with theory (Reynolds & Elrick, 1990).

For each layered soil (weakly, moderately, and strongly), Figure 3 shows the infiltration rate curves corresponding to the three thickness values of the upper layer ($t_{ul} = 0.5$, 1, and 3 cm) together with those for the two homogeneous soils that were combined with each other to form the layered soil. Generally, the infiltration rates of the layered soil approached more the i_r values of the homogeneous SIL soil than those of

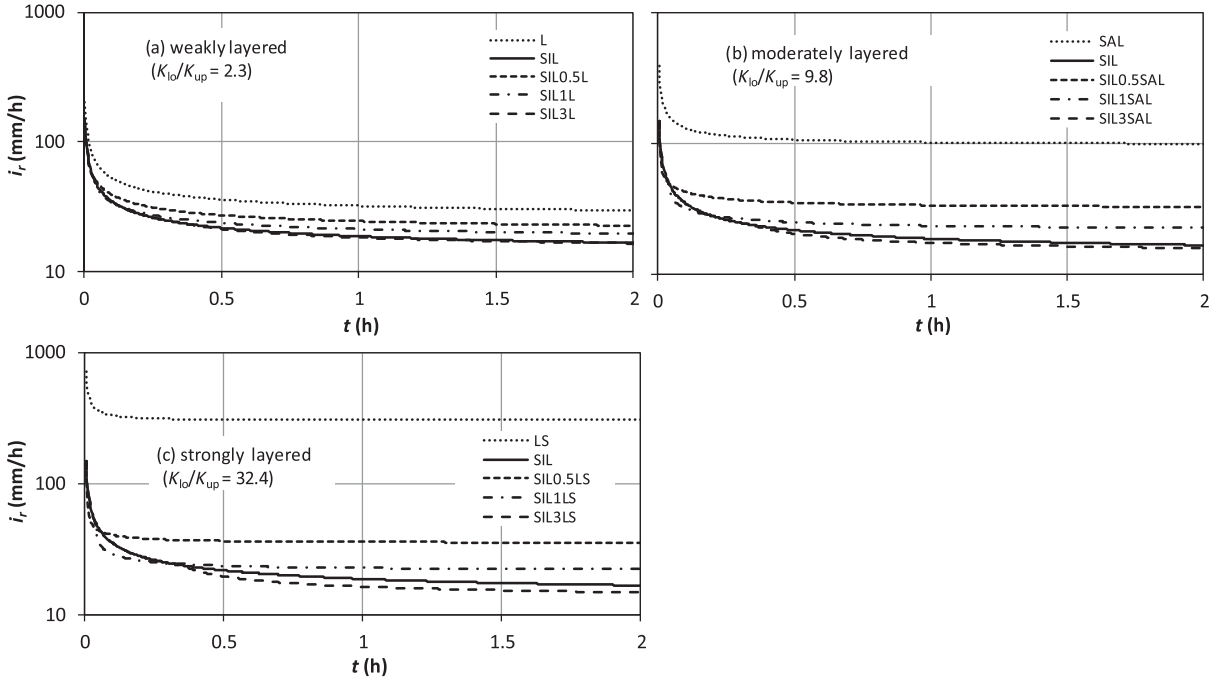

FIGURE 3 Infiltration rates, i_r, for the homogeneous SIL (silt-loam), L (loam), SAL (sandy-loam), and LS (loamy-sand) soils and the layered soils plotted against time, t. (a) SIL overlying L (weakly layered soil); (b) SIL overlying SAL (moderately layered soil); (c) SIL overlying LS (strongly layered soil). K_{lo}/K_{up}, K_s of the lower layer/K_s of the upper layer.

the homogeneous coarser soil constituting the subsoil in the layered system (L, SAL, and LS, depending on the scenario). In particular, for a weak layering (SIL over L), the differences between the layered soil and the coarser soil did not differ very much from those between the layered soil and the finer soil given that two corresponding infiltration rates (layered vs. homogeneous) differed by 1.3–1.8 times during the run in the former case and by 1.0–1.4 times in the latter one. This result occurred since infiltration rates for the homogeneous SIL and L soils were relatively similar (Figures 2 and 3). Instead, in the case of a strong layering (SIL over LS), the layered soil yielded i_r values differing by 4.9–20.7 and 1.0–2.1 times as compared with the coarser and the finer soil, respectively. Intermediate results were obtained for the moderately layered soil (SIL over SAL) since, in this case, infiltration rates differed by 2.7–6.3 times from those of the coarser soil and by 1.0–2.0 times as compared with the finer soil.

Therefore, the layered soils showed a greater similarity with the SIL soil of the upper layer than the coarser soils below. This result became more and more clear as the thickness of the upper layer increased (Figure 3), as expected, but it was also detected with a very thin upper layer (0.5 cm).

After 2 h of infiltration, 0.5 cm of SIL induced a decrease in the final infiltration rate, i_{rf}, by 1.3 times when this layer was positioned over the L soil, 3.0 times when the subsoil was a SAL soil and 8.6 times with the LS soil as the subsoil (Table 3). Therefore, a thin upper layer of a fine soil had a larger effect on i_{rf} as the subsoil was coarser. Final infiltration rates of the three homogeneous coarse soils (L, SAL, and LS) differed by 10.3 times (29.6–304.4 mm/h). The presence of a thin layer of a fine soil on these three soils determined a shift of the range of i_{rf} toward smaller (22.6–35.4 mm/h) and less variable (ratio between the highest and the lowest i_{rf} value = 1.6) values. Conversely, the thin layer of SIL soil over a coarser soil yielded higher i_{rf} values for the layered soil than the homogeneous SIL soil (Table 3). The increase in i_{rf} was greater as the layering degree increased (from 1.4 times for the SIL0.5L soil to 2.1 times for the SIL0.5LS soil).

Therefore, for a weak layering degree, the i_{rf} value of the layered soil was almost equally distant from the i_{rf} values of the two associated homogeneous soils (SIL0.5L soil: 1.3 times smaller as compared with the L soil and 1.4 times greater as compared with the SIL soil). A stronger layering enhanced the differences between the layered soil and the two associated homogeneous soil but more appreciably with reference to the differences with the coarser soil than the finer soil (SIL0.5LS soil: 8.6 times smaller i_{rf} value as compared with the LS soil and 2.1 times greater i_{rf} value as compared with the SIL soil).

As logical, a greater thickness of the upper SIL layer enhanced similarities between the layered and the homogeneous SIL soils and differences between the layered and the homogeneous coarser soils (Table 3). Some results did not appear fully intuitive. For example, as compared with the homogeneous SIL soil, the presence of a coarser subsoil

TABLE 3 Differences between the final infiltration rates, i_{rf}, in the layered and the homogeneous soils expressed as the ratio between the highest and the lowest i_{rf} values.

Layered soil	Thickness of the upper layer (cm)	Final infiltration rate[a], i_{rf} (mm/h)	Factor of difference	
			As compared with the homogeneous coarser soil	As compared with the homogeneous finer soil
SIL over L	0.5	22.6	1.31	1.36
	1	19.5	1.51	1.17
	3	16.5	1.79	1.01
SIL over SAL	0.5	32.7	3.04	1.97
	1	22.6	4.40	1.36
	3	15.8	6.31	1.06
SIL over LS	0.5	35.4	8.59	2.13
	1	22.2	13.7	1.33
	3	14.7	20.7	1.13

[a]Final infiltration rates, i_{rf}, of the homogeneous soils equal to 16.6, 29.6, 99.4, and 304.4 mm/h for the SIL (loamy-sand), L (loam), SAL (sandy-loam), and LS (loamy-sand) soils, respectively.

below 3 cm of SIL soil reduced i_{rf} by a little, but more appreciably as the subsoil became coarser (i_{rf} = 16.6 mm/h for the SIL soil and 16.5, 15.8, and 14.7 mm/h for the SIL3L, SIL3SAL, and SIL3LS soils, respectively).

3.1.2 | Infiltration rate ratios

For each layered soil (SIL over L, SIL over SAL, and SIL over LS), Figure 4a–c shows $i_{r\mathrm{LH}}$ versus t for the three t_{ul} values (0.5, 1, and 3 cm). The same data were reported in Figure 4d–f by plotting, for each t_{ul} value, $i_{r\mathrm{LH}}$ versus t for the three layering degrees. The following sequence of four stages was generally detected for the $i_{r\mathrm{LH}}$ versus t relationships: stage 1, $i_{r\mathrm{LH}} = 1$; stage 2, $i_{r\mathrm{LH}} < 1$, decreasing as t increased; stage 3, $i_{r\mathrm{LH}} < 1$, increasing as t increased; stage 4, $i_{r\mathrm{LH}} > 1$, increasing with time. Therefore, a stage was defined by simultaneously considering the values of $i_{r\mathrm{LH}}$ (<1, = 1, >1) and the variation of these values with time (increasing, decreasing). For t_{ul} = 3 cm, the last stage was not detected and stage 3 was only weakly perceived. Evidently, stage 1 corresponded to the early phase of the infiltration process, during which the characteristics of the flow field did not change between the layered and the homogeneous soil. As logical, the duration of stage 1 increased with the thickness of the upper soil layer nearly independently of the underlying coarser soil since this duration was 0.2 min for a thickness of 0.5 cm, 1.6 min for a thickness of 1 cm, and 18.8–19.4 min for a thickness of 3 cm (Table 4). As infiltration started to occur in the underlying coarser soil, the infiltration rates became smaller as compared with those of the homogeneous SIL soil. This slowdown reached a maximum (smallest $i_{r\mathrm{LH}}$ value) and then it decreased since, from a certain instant, $i_{r\mathrm{LH}}$ started to steadily increase. Due to this increase, infiltration later became faster in the layered soil than in the homogeneous SIL soil. The thinner the upper layer, (i) the smaller the lowest $i_{r\mathrm{LH}}$ value during stages 2 and 3 ($i_{r\mathrm{LH}} < 1$) (Figure 4a–c), (ii) the higher the greatest $i_{r\mathrm{LH}}$ value during stage 4 ($i_{r\mathrm{LH}} > 1$), and (iii) the shortest the duration of stages 2 and 3 (Table 4). For a given thickness of the upper soil layer, the coarser the subsoil, (i) the lower the minimum $i_{r\mathrm{LH}}$ value during stages 2 and 3 (Figure 4d–f) and (ii) the longer the duration of these two stages (Table 4).

Therefore, in comparison with the infiltration rates of a homogeneous fine soil, those of a layered soil composed of an upper fine soil layer overlying a coarser soil evolved according to the following sequence: (i) identical, (ii) smaller and decreasing, (iii) smaller and increasing, and (iv) greater and increasing. This trend had an impact on cumulative infiltration, I, as shown in the example of Figure 5 for a thickness of the upper fine soil layer equal to 1 cm. In particular, the I values of the homogeneous and layered soils coincided during stage 1 and also later, but only at a single instant in this case. At this particular instant, there was a balance between the decreased infiltration rates during stages 2 and 3 and the increased infiltration rates during stage 4. The coarser the soil underlying the upper layer, the later this instantaneous condition of equality of I was reached.

According to this investigation, the conclusion by Lassabatere et al. (2010) and da Silva Ribas et al. (2021) can be formulated in a little greater detail. In particular, the suggestion by these authors was supported but it is also necessary to specify that, for a little permeable upper layer, the similarity between the layered soil and the homogeneous fine soil depends on both the thickness of the upper layer and the hydraulic properties of the subsoil. Similarity generally increases with a thicker upper layer. In the case of a weak layering, the layered soil is expected to yield an

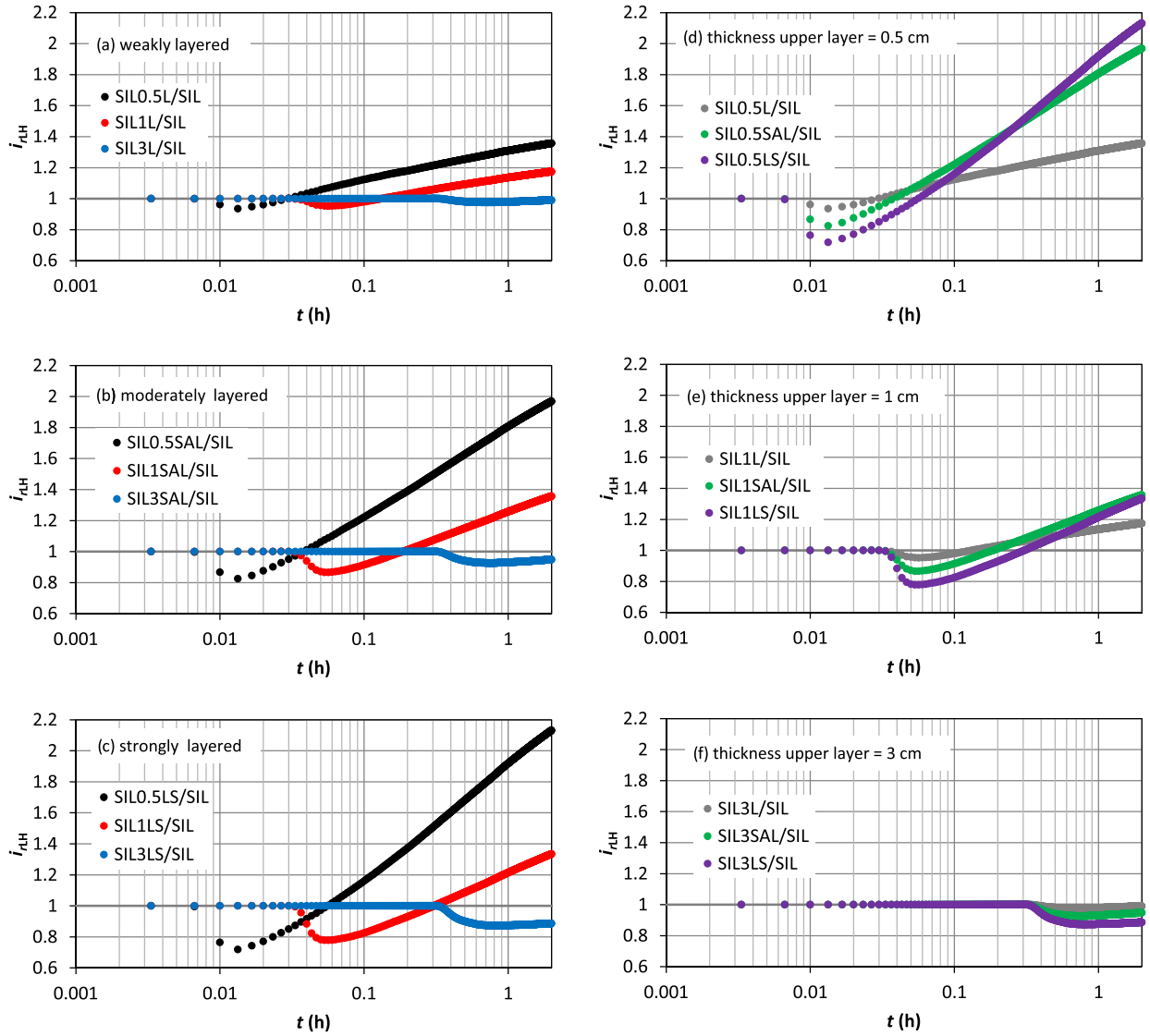

FIGURE 4 Infiltration rate ratios, i_{rLH} (layered/homogeneous SIL [silt-loam] soil), plotted against time, t, for a weakly (a), moderately (b), and strongly (c) layered soil and for a thickness of the upper layer equal to 0.5 cm (d), 1 cm (e), and 3 cm (f). L, loam; LS, loamy-sand; SAL, sandy-loam.

TABLE 4 Duration (min) of the infiltration run in the layered soil yielding equal (1), smaller (<1), and larger (>1) infiltration rates as compared with the infiltration rate of the homogeneous SIL soil for the three layered soils and the three thickness values of the upper soil layer.

		Thickness of the upper layer (cm)		
Layered soil	**Infiltration rate ratio (layered/SIL soils)**	**0.5**	**1**	**3**
SIL over L	1	0.2	0.2–1.6	0.2–19.4
	<1	0.4–1.6	1.8–8.0	≥19.6
	>1	≥1.8	≥8.2	
SIL over SAL	1	0.2	0.2–1.6	0.2–18.8
	<1	0.4–2.2	1.8–11.2	≥19.0
	>1	≥2.4	≥11.4	
SIL over LS	=1	0.2	0.2–1.6	0.2–18.8
	<1	0.4–3.2	1.8–18.4	≥19.0
	>1	≥3.4	≥18.6	

Abbreviations: L, loam; LS, loamy-sand; SIL, silt-loam; SAL, sandy-loam.

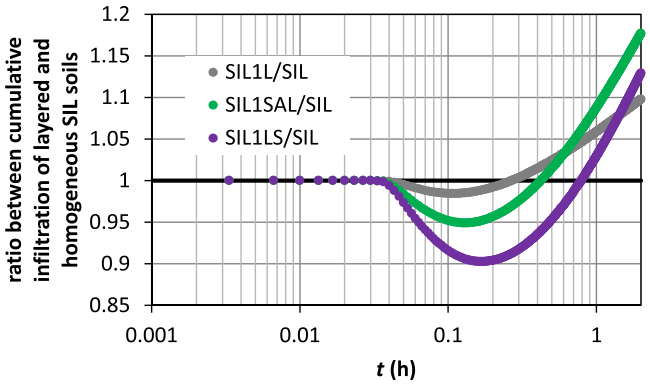

FIGURE 5 Ratio between the cumulative infiltration of the layered soil and that of the homogeneous SIL soil plotted against time, *t*. L, loam; LS, loamy-sand; SAL, sandy-loam; SIL, silt-loam.

intermediate infiltration as compared with that for the two homogeneous soils that form the layered system. If the layering degree is strong, the layered soil appears more similar to the homogeneous fine soil than to the homogeneous coarse soil.

3.1.3 | Cumulative infiltration

For each layering degree, Figure 6 compares the cumulative infiltration curves for the two homogeneous soils that were combined with each other to form the layered soil with three different thicknesses of the upper layer ($t_{ul} = 0.5$, 1, and 3 cm). Cumulative infiltration was obviously greater in the homogeneous coarse soils (L, SAL, and LS) than the homogeneous SIL soil. As expected, differences between two homogeneous soils were relatively small for the L–SIL comparison (ratio between I at $t = 0.5$ h equal to 1.5), intermediate for the SAL–SIL comparison (ratio = 3.9), and relatively high in the case of the LS–SIL comparison (ratio = 10.2).

Regardless of both the degree of layering and the thickness of the upper SIL layer, the cumulative infiltration curves of the layered soils were closer to that of the homogeneous SIL soil than to the cumulative infiltration curve of the homogeneous soil constituting the coarser subsoil in the layered system. In the representations of Figure 6, the overlap of the infiltration curves of the homogeneous SIL soil and the layered soils appeared more complete for $t_{ul} = 1$ and 3 cm than $t_{ul} = 0.5$ cm. In this last case, with the exclusion of the early stage of the run, more water infiltrated in the layered soil than in the homogeneous SIL soil.

According to Yilmaz et al. (2013), inverse numerical modeling of the infiltration data obtained in a two-layered system with a less permeable upper layer should be expected to yield representative hydraulic parameters of the upper layer. The results of this investigation appeared to agree with the conclusion by Yilmaz et al. (2013) given the appreciable overlap between the infiltration corresponding to the homogeneous SIL soil and those obtained for the layered soils, regardless of the layering degree and especially for $t_{ul} \geq 1$ cm.

The time evolution of percent differences between cumulative infiltration of the layered and homogeneous SIL soils, ΔI_{LH}, for the nine layered soils is shown in Figure 7. Similarity between the layered soils and the SIL soil generally increased with the thickness of the upper layer, as expected, since $-11.1\% \leq \Delta I_{LH} \leq +29.5\%$, $-9.7\% \leq \Delta I_{LH} \leq +2.4\%$, and $-1.4\% \leq \Delta I_{LH} \leq 0$ were obtained for $t_{ul} = 0.5$, 1, and 3 cm, respectively. With a small thickness of the upper layer (0.5 cm), $I_{layered} > I_{SIL}$ (positive ΔI_{LH} values) was the most frequent result during the run. The opposite result ($I_{layered} < I_{SIL}$ for the largest part of the run) was obtained with an intermediate thickness (1 cm), especially with reference to a moderate and strong layering condition. Finally, $I_{layered} = I_{SIL}$ prevailed with the thickest upper layer (3 cm). Weaker layering conditions generally made infiltration for the layered soil more similar to that of the homogeneous SIL soil, regardless of the thickness of the upper layer. A thicker upper soil generally made infiltration in layered soil more similar to that of the homogeneous SIL soil, regardless of the layering degree.

3.1.4 | Sequential analysis procedure

The infiltration model was adapted to the data for $t \geq 0.17$ h, that is, by considering at least 10 data points for the fitting, which yielded 21 RMSE values for a run. Calculations of RMSE were performed for the homogeneous SIL soil and the SIL3L, SIL3SAL, and SIL3LS layered soils. The sequential analysis was not applied for small t_{ul} values (≤1 cm) since, in this case, the wetting front reached the interface between the two layers very soon (≤1.6 min, Table 4), meaning that RMSE values representative of the upper layer alone could not be obtained. Instead, for $t_{ul} = 3$ cm, the first 17 RMSE values ($t \leq 0.283$ h) were obtained in the upper layer, whereas the last 13 values represented infiltration in the two-layered system.

For the homogeneous SIL soil, the RMSE versus t relationship described a curve concave downward, denoting that RMSE increased regularly with time at a decreasing rate as t increased (Figure 8a). An increasing RMSE versus t relationship was also detected in the presence of the subsoil. However, approximately starting from the time at which infiltration also occurred in the subsoil, RMSE became higher for the layered soils than the homogeneous SIL soil, as expected (Moret-Fernández et al., 2021). This increase in RMSE was minimal in the case of a weakly layered soil (SIL3L) and more appreciable as the layering degree increased.

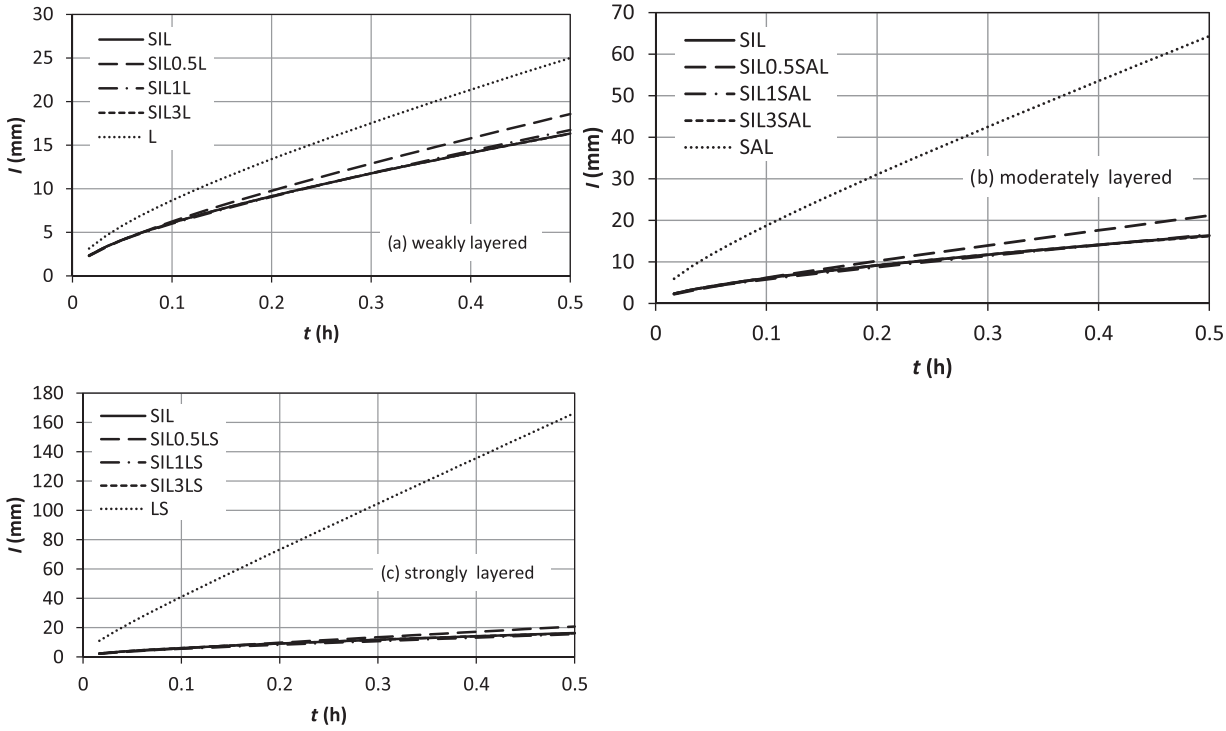

FIGURE 6 Cumulative infiltration, I, for the homogeneous SIL (silt-loam), L (loam), SAL (sandy-loam), and LS (loamy-sand) soils and the layered soils plotted against time, t. (a) SIL overlying L (weakly layered soil); (b) SIL overlying SAL (moderately layered soil); and (c) SIL overlying LS (strongly layered soil).

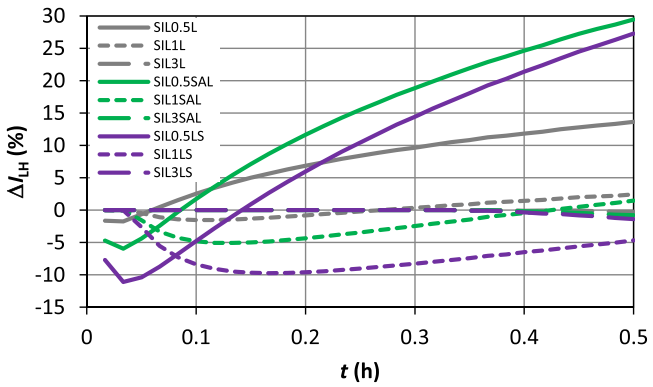

FIGURE 7 Percent difference between cumulative infiltration of the layered and homogeneous SIL (silt-loam) soils, ΔI_{LH}, plotted against time, t, for the different layering degrees and thickness values of the upper soil layer. L, loam; LS, loamy-sand; SAL, sandy-loam.

Despite the detected differences between the homogeneous and the layered soils, the usability of the RMSE versus t relationship to determine the time when the infiltration bulb reaches the interface between the upper soil layer and the subsoil appeared somehow questionable for a twofold reason: (i) the general shape of the RMSE(t) curve did not change substantially between homogeneous and layered soils, and (ii) field data are unavoidably more noised than those used for this analysis. Therefore, layering could be difficult to be detected in practice from the RMSE versus t relationship.

However, analyzing the same data, that is, RMSE and t, in an alternative manner was found to make detection of soil layering conditions easier. In particular, Figure 8b shows ΔRMSE/Δt plotted against the duration of the infiltration run. In the case of the homogeneous SIL soil, ΔRMSE/Δt decreased monotonically and the relationship between this ratio and t was concave upward. For both a moderately and a strongly layered soil, after a decreasing stage denoting infiltration in the upper layer, ΔRMSE/Δt increased rather abruptly and then it started to decrease again after reaching a maximum. The time at which the increase in ΔRMSE/Δt became detectable was very close to the time when infiltration started to occur in the subsoil (difference by no more than 1–2 min), suggesting that ΔRMSE/Δt started to increase because the subsoil started to influence infiltration. The results were less clear for a weakly layered soil due to the lack of a well-defined peak in the ΔRMSE/Δt versus t plot. However, even in this case, a departure of the ΔRMSE/Δt versus t relationship from that obtained for the homogeneous SIL soil appeared perceivable.

Therefore, the sequential analysis procedure first introduced by Moret-Fernández et al. (2021) appears usable to detect layering conditions. However, according to this investigation, infiltration rates should be considered, the Horton (1940) infiltration model should be fitted to the data and the relationship between ΔRMSE/Δt and t should be examined. A concave upward relationship between these two variables is

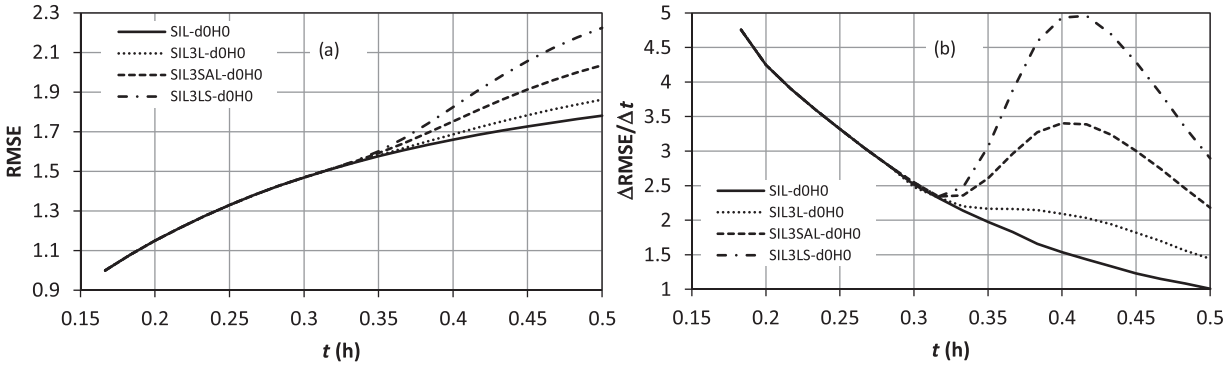

FIGURE 8 Plot of the root mean square, RMSE (mm/h), versus time, *t*, data according (a) to Moret- Fernández et al. (2021) and (b) the modified sequential analysis procedure. L, loam; LS, loamy-sand; SAL, sandy-loam; SIL, silt-loam.

expected for a homogeneous soil. A moderate or strong layering condition is signaled by a sharp increase in the $\Delta RMSE/\Delta t$ versus t relationship after a decreasing stage. For a weakly layered soil condition, an alteration of the regularity of the $\Delta RMSE/\Delta t$ versus t curve could represent all that it is possible to detect. In other words, the effectiveness of the suggested procedure appears to depend on the layering degree, being not surprisingly highest in the case of strong layering degrees.

3.2 | Comparing the d0H0 and d1H1 setups

3.2.1 | Infiltration rates

With reference to a 2-h infiltration run sampled at $\Delta t = 1$ min time intervals, Figure 9 shows, for the three-layered soils and the three t_{ul} values for each layering degree, the relationship between Δi_{rPT}, that is, the percentage difference between the i_r values for the d1H1 and d0H0 setups, and t. The Δi_{rPT} values obtained for the homogeneous SIL soil were also reported in the figure. The individual Δi_{rPT} values varied from a minimum of −18.8% (SIL3LS soil) to a maximum of +17.4% (SIL0.5LS soil), and the means of Δi_{rPT} varied from −10.4% (SIL soil), or −9.9% (SIL3L soil) by only considering the layered soils, to +16.1% (SIL0.5LS soil). Therefore, the effect of the setup on i_r was overall small or moderate.

For the homogeneous SIL soil, Δi_{rPT} was < 0 for the entire run duration (from −15.0% to −4.4%), meaning that i_r(d1H1) was steadily smaller than i_r(d0H0). In other terms, the d1H1 setup determined a slower infiltration process than the d0H0 setup, as already reported by Bagarello et al. (2022).

Although Δi_{rPT} fell into a not very broad range of values, the layering degree influenced the Δi_{rPT} calculations. In particular, $-15.0\% \le \Delta i_{rPT} \le +2.6\%$, $-16.7\% \le \Delta i_{rPT} \le +12.9\%$, and $-18.8\% \le \Delta i_{rPT} \le +17.4\%$ were obtained for the SIL-L, SIL-SAL, and SIL-LS soils, respectively, denoting a wider range for a stronger layering. As expected, the greatest similarity between the Δi_{rPT} values calculated for the homogeneous SIL soil and those obtained for the layered soils was detected in the case of the thickest upper layer (t_{ul} = 3 cm), regardless of the layering degree. In particular, the overlap of the two Δi_{rPT}(t) curves was initially complete, which was obvious since flow fields initially coincided. Then, an effect of the subsoil was detected since the overlap of the two curves persisted in the case of a weak layering (SIL3L soil) but not, or at least less clearly, in the case of a moderate and strong layering (SIL3SAL and SIL3LS soils, respectively). The decrease in t_{ul} made the difference between the results for the layered and the homogeneous SIL soils more appreciable since it generally determined an increase in Δi_{rPT} for the layered soils that became less negative or even positive, depending on the layering degree. In particular, a thin upper layer (t_{ul} = 0.5 cm) yielded a mean of Δi_{rPT} nearly null (−0.2%) and individual Δi_{rPT} values close to or not very different from zero (from −5.7% to +2.6%) for a weak layering. For a moderate and a strong layering, the individual Δi_{rPT} values and the corresponding means were > 0 (from +0.3% to +12.9% and +10.9% in the former case; from +2.0% to +17.4% and +16.1% in the latter one).

For the homogeneous SIL soil, the final infiltration rate, i_{rf}, obtained with the practical setup (d1H1) was smaller by 7.4% than the corresponding value obtained with the theoretical setup (d0H0). With reference to the layered soils, Δi_{rfPT}, that is, the percentage difference between corresponding i_r values with the two setups at the end of the 2-h run, varied from −6.5% to +17.4%. In particular, the conditions determining the greatest differences between the d0H0 and d1H1 setups ($\Delta i_{rfPT} \ge +13.0\%$) were those of a moderately or strongly layered soil and a thin (0.5 cm) upper layer. The best similarity between the two setups ($-0.4\% \le \Delta i_{rfPT} \le +2.6\%$) was detected for a weakly layered soil and a thin or relatively thin (0.5–1 cm) upper layer.

Therefore, this analysis suggested that, with a thick upper layer, the results should not be expected to differ greatly between the layered soil and the homogeneous SIL soil, regardless of the layering degree. In particular, smaller

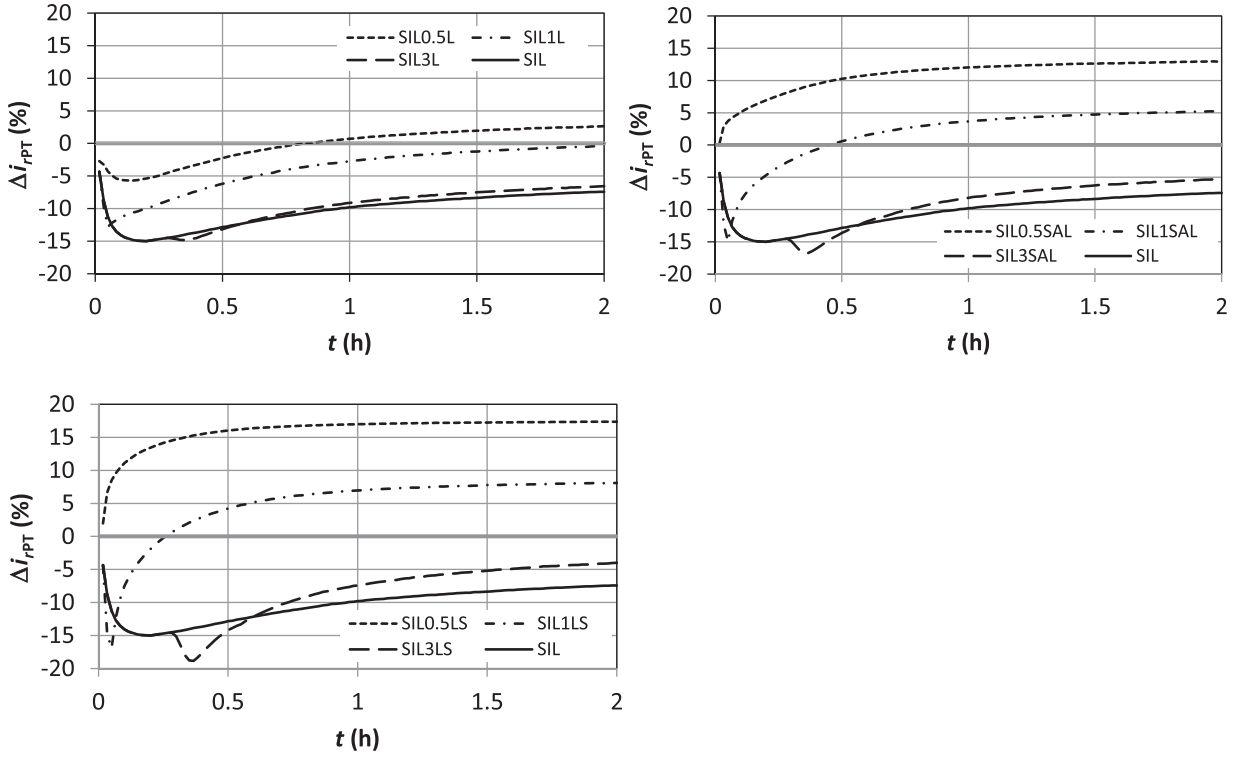

FIGURE 9 Percent difference between infiltration rate for the practical (d1H1) and the theoretical (d0H0) setup, Δi_{rPT}, plotted against time, t, for the different layering degrees and thicknesses of the upper soil layer. L, loam; LS, loamy-sand; SAL, sandy-loam; SIL, silt-loam.

infiltration rates are expected with the practical setup (d1H1) as compared with the theoretical one (d0H0). If the upper layer is thin, the impact of the layering degree becomes more appreciable. For a weak layering degree, i_r(d1H1) ≈ i_r(d0H0) appears a plausible assumption. For moderate or strong degrees of layering, i_r(d1H1) > i_r(d0H0) appears more likely. In other words, layering may make theoretical (d0H0) and practical (d1H1) infiltration rates like each other. This situation is expected to occur in the case of a weak layering and a thin upper layer.

3.2.2 | Cumulative infiltration

Figure 10 shows the percent differences, ΔI_{PT}, between the cumulative infiltration values obtained with the d1H1 and d0H0 setups during the 0.5 h-run. The ΔI_{PT} values varied in the rather narrow range of $-12.2\% \le \Delta I_{PT} \le +11.8\%$, denoting an overall limited effect of the used setup on cumulative infiltration. As expected in accordance with the infiltration rate calculations (Figure 9), the setup effect for a thick upper layer (t_{ul} = 3 cm) was similar to that observed for the homogeneous SIL soil, meaning that, regardless of the layering degree, cumulative infiltration for the d1H1 setup was up to about 11%–12% lower than that obtained with the d0H0 setup. A layering degree effect was instead perceived with a thin upper layer (t_{ul} = 0.5 cm). In particular, a weak layering implied detecting I(d1H1) < I(d0H0) albeit by only a little given that ΔI_{PT} was not smaller than −4.0%. Instead, I(d1H1) > I(d0H0) was obtained with a moderate and a strong layering but only by a little also in these cases since ΔI_{PT} did not exceed +6.4% in the former case and +11.8% in the latter one. With an upper layer of an intermediate thickness (t_{ul} = 1 cm), $\Delta I_{PT} \le 0$ was obtained. In particular, for a weak layering, ΔI_{PT} stabilized around a value of nearly −8.0% as the duration of the run increased up to 0.5 h. For a moderate and a strong layering, ΔI_{PT} reached a minimum of nearly −7.0% and then it started to increase, remaining negative.

Therefore, the correspondence between the two setups differed depending on both the layering degree and the thickness of the upper layer. Less cumulative infiltration occurred with the d1H1 setup than the d0H0 one for an upper layer of intermediate to high thickness and also for a thin upper layer but only in the case of a weak layering degree. Otherwise, the practical setup yielded more cumulative infiltration than the theoretical one.

While d = 1 cm represents a common practice of the Beerkan infiltration run, establishing a constant H value equal to 1 cm represented a rather extreme case for such a type of run. Other scenarios that should perhaps be tested in the future are as follows: (i) positive, constant, and smaller H values (e.g., <0.5 cm), as those established with the automated infiltrometer by Di Prima (2015); and (ii) decreasing ponded depths of water for each water volume application (e.g., from

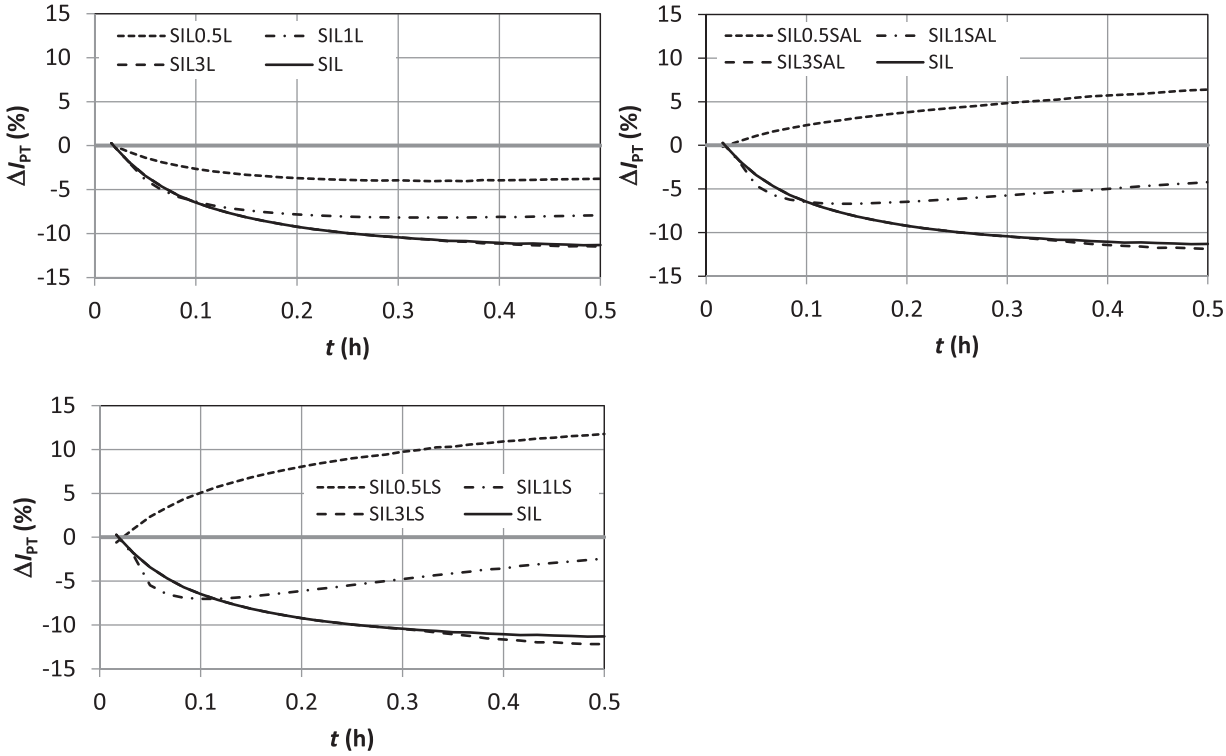

FIGURE 10 Percentage difference between cumulative infiltration for the practical (d1H1) and the theoretical (d0H0) setup, ΔI_{PT}, plotted against time, t, for the different layering degrees and thicknesses of the upper soil layer. L, loam; LS, loamy-sand; SAL, sandy-loam; SIL, silt-loam.

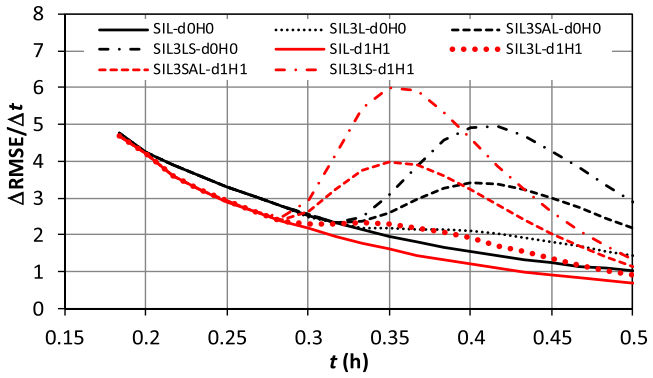

FIGURE 11 Comparison of the ΔRMSE/Δt versus t (where RMSE is the root mean square error in mm/h and t is the time in h) relationships for the practical (d1H1) and the theoretical (d0H0) setups.

0.8–1.1 to 0 cm), in accordance with Lassabatere et al. (2006) and Xu et al. (2012).

3.2.3 | Sequential analysis procedure

Figure 11 compares the ΔRMSE/Δt curves for the d0H0 and d1H1 setups. The general shape of this curve did not change between these two setups. However, the increasing phase of the ΔRMSE/Δt versus t relationship was detected earlier with the practical setup than the theoretical one. This result was consistent with the circumstance that the infiltration rates for the layered and the homogeneous SIL soils started to diverge a little earlier with the d1H1 setup (approximately after 16–17 min) than with the d0H0 setup (after nearly 19 min). The increase in the curve appeared sharper for the practical setup than the theoretical one and the largest vertical amplitude of the ΔRMSE/Δt versus t curves, defined as the largest distance between the ΔRMSE/Δt versus t curves for the layered and the homogeneous SIL soils, increased from the d0H0 setup (0.6–3.5 units, depending on the layered soil) to the d1H1 one (0.7–4.5 units). Therefore, the practical setup induced in general a more clearly detectable departure of the ΔRMSE/Δt versus t curve from the one corresponding to the homogeneous SIL soil. In other words, the practical setup enhanced the possibility to recognize the time at which the characteristics of the subsoil started to influence the infiltration process.

4 | CONCLUSIONS

In this investigation, infiltration in a layered soil with a less permeable upper layer and a more permeable subsoil was numerically studied for both a theoretical process with null depth of ring insertion, d, and ponded head of water, H (d0H0 setup), and an approximation of this process, obtained with $d = H = 1$ cm (practical setup, d1H1). The considered

layered soils differed by both the layering degree (from weak to strong) and the thickness of the upper soil layer (0.5–3 cm). A fixed source size (radius = 5 cm) and a constant antecedent soil water pressure head (−9022 cm) were considered for simulating infiltration.

It was concluded that water infiltration is more representative of the upper soil layer when this layer is the less permeable. In particular, infiltration rates for the layered soil can be expected to be greater than those of the homogeneous little permeable soil by no more than nearly two times but they can also be ∼20 times smaller than those of the homogeneous coarser soil that constitutes the subsoil. For a weak layering condition, the layered soil yields an intermediate infiltration as compared with that of the two homogeneous soils forming the layered system. For a strong layering degree, the layered soil is more similar to the homogeneous fine soil than to the homogeneous coarse soil.

Using the practical setup (d1H1) instead of the theoretical one (d0H0) should have a small to moderate effect on the instantaneous infiltration rates since they can be expected to vary with the setup by nearly 20% at the most.

A sequential analysis procedure appears usable to detect layering conditions but with some modifications as compared with the originally proposed procedure. In particular, an empirical model is fitted to infiltration rate values. The effectiveness of the method seems to depend on the layering degree, being not surprisingly highest in the case of strong layering degrees. The practical setup appears to enhance the possibility to recognize the time at which the characteristics of the subsoil start to influence the infiltration process with the modified sequential analysis procedure.

This investigation tried to take a small and incomplete step forward as regards the transition from the ideal conditions to the real ones. In this context, this investigation could represent the starting point of additional developments in the study of 3D infiltration into a soil composed of a little permeable upper layer and a coarser subsoil. In particular, the fact that some results of this investigation were not intuitive demonstrates the opportunity of the investigation that was carried out and indicates the need for further developments. Simultaneously considering infiltration and soil water pressure heads in the wetted zone could help to generally improve description of 3D infiltration in layered soils. Moreover, layering and setup effects should be studied by also considering different sizes of the source, different antecedent soil water conditions, and also soil heterogeneity. Numerical simulation could be an appropriate tool at these purposes since different relevant data, such as those on water content of the wetted soil volume, lateral expansion of this volume, and pressure heads in different points of the wetted soil, can be obtained with a great detail. It should also be considered that, in the field, a single soil layer is not homogeneous, rigid, and isotropic. Therefore, numerical simulations should be performed by improving soil description, maybe step by step, in an attempt to get as close as possible to a realistic description of the porous medium. Finally, another objective that perhaps should be pursued is trying to better define potential and limitations of the sequential analysis procedure, at least from the perspective to detect the presence of layering with a simple infiltration experiment.

AUTHOR CONTRIBUTIONS

Vincenzo Bagarello: Conceptualization; investigation; writing—original draft. **Massimo Iovino**: Conceptualization; investigation; writing—original draft. **Jianbin Lai**: Conceptualization; investigation; writing—original draft.

ACKNOWLEDGMENTS

This study was carried out within the RETURN Extended Partnership and received funding from the European Union Next-GenerationEU (National Recovery and Resilience Plan–NRRP, Mission 4, Component 2, Investment 1.3–D.D. 1243 2/8/2022, PE0000005). It is also supported by the National Natural Science Foundation of China (Grant no. U22A20555).

CONFLICT OF INTEREST STATEMENT

The authors declare no conflicts of interest.

ORCID

Massimo Iovino https://orcid.org/0000-0002-3454-2030
Jianbin Lai https://orcid.org/0000-0002-9725-9283

REFERENCES

Alagna, V., Bagarello, V., Di Prima, S., Guaitoli, F., Iovino, M., Keesstra, S., & Cerdà, A. (2019). Using Beerkan experiments to estimate hydraulic conductivity of a crusted loamy soil in a Mediterranean vineyard. *Journal of Hydrology and Hydromechanics*, *67*(2), 191–200. https://doi.org/10.2478/johh-2018-0023

Angulo-Jaramillo, R., Bagarello, V., Di Prima, S., Gosset, A., Iovino, M., & Lassabatere, L. (2019). Beerkan Estimation of Soil Transfer parameters (BEST) across soils and scales. *Journal of Hydrology*, *576*, 239–261. https://doi.org/10.1016/j.jhydrol.2019.06.007

Angulo-Jaramillo, R., Bagarello, V., Iovino, M., & Lassabatere, L. (2016). *Infiltration measurements for soil hydraulic characterization*. Springer International Publishing. https://doi.org/10.1007/978-3-319-31788-5

Assouline, S. (2004). Rainfall-induced soil surface sealing: A critical review of observations, conceptual models, and solutions. *Vadose Zone Journal*, *3*(2), 570–591. https://doi.org/10.2136/vzj2004.0570

Assouline, S., & Mualem, Y. (1997). Modeling the dynamics of seal formation and its effect on infiltration as related to soil and rainfall characteristics. *Water Resources Research*, *33*(7), 1527–1536.

Assouline, S., & Mualem, Y. (2002). Infiltration during soil sealing: The effect of areal heterogeneity of soil hydraulic properties. *Water Resources Research*, *38*(12), 22-1–22-9. https://doi.org/10.1029/2001WR001168

Assouline, S., Tessier, D., & Tavares-Filho, J. (1997). Effect of compaction on soil physical and hydraulic properties:

Experimental results and modeling. *Soil Science Society of America Journal*, *61*, 390–398. https://doi.org/10.2136/sssaj1997.03615995006100020005x

Bagarello, V., Di Prima, S., & Iovino, M. (2014). Comparing alternative algorithms to analyze the Beerkan infiltration experiment. *Soil Science Society of America Journal*, *78*, 724–736. https://doi.org/10.2136/sssaj2013.06.0231

Bagarello, V., Dohnal, M., Iovino, M., & Lai, J. (2022). Correspondence between theory and practice of a Beerkan infiltration experiment. *Vadose Zone Journal*, *21*, e20220. https://doi.org/10.1002/vzj2.20220

Bagarello, V., Iovino, M., & Lai, J. (2019). Accuracy of saturated soil hydraulic conductivity estimated from numerically simulated single-ring infiltrations. *Vadose Zone Journal*, *18*, 01–12. https://doi.org/10.2136/vzj2018.06.0122

Batey, T. (2009). Soil compaction and soil management–A review. *Soil Use and Management*, *25*, 335–345. https://doi.org/10.1111/j.1475-2743.2009.00236.x

Ben-Hur, M., Shainberg, I., & Morin, J. (1987). Variability of infiltration in a field with surface-sealed soil. *Soil Science Society of America Journal*, *51*, 1299–1302. https://doi.org/10.2136/sssaj1987.03615995005100050037x

Carsel, R. F., & Parrish, R. S. (1988). Developing joint probability distributions of soil water retention characteristics. *Water Resources Research*, *24*, 755–769.

Close, K. R., Frasier, G., Dunn, G. H., & Loftis, J. C. (1998). Tension infiltrometer contact interface evaluation by use of a potassium iodide tracer. *Transactions of the ASAE*, *41*, 995–1004.

da Silva Ribas, L. V., Coutinho, A. P., Lassabatere, L., Neto, S. M. D. S., Montenegro, S. M. G. L., De Gusmão Da Cunha Rabelo, A. E. C., Jaramillo, R. A., & Neto, A. R. (2021). Effect of the choice of different methods on the permeable pavement hydraulic characterization and hydrological classification. *Journal of Hydrology and Hydromechanics*, *69*(3), 332–346. https://doi.org/10.2478/johh-2021-0018

Di Prima, S. (2015). Automated single ring infiltrometer with a low-cost microcontroller circuit. *Computers and Electronics in Agriculture*, *118*, 390–395. https://doi.org/10.1016/j.compag.2015.09.022

Di Prima, S., Concialdi, P., Lassabatere, L., Angulo-Jaramillo, R., Pirastru, M., Cerdà, A., & Keesstra, S. (2018). Laboratory testing of Beerkan infiltration experiments for assessing the role of soil sealing on water infiltration. *Catena*, *167*, 373–384. https://doi.org/10.1016/j.catena.2018.05.013

Dohnal, M., Vogel, T., Dusek, J., Votrubova, J., & Tesar, M. (2016). Interpretation of ponded infiltration data using numerical experiments. *Journal of Hydrology and Hydromechanics*, *64*, 289–299.

Dušek, J., Dohnal, M., & Vogel, T. (2009). Numerical analysis of ponded infiltration experiment under different experimental conditions. *Soil & Water Research*, *4*, S22–S27.

Haverkamp, R., Ross, P. J., Smettem, K. R. J., & Parlange, J. Y. (1994). Three-dimensional analysis of infiltration from the disc infiltrometer: 2. Physically-based infiltration equation. *Water Resources Research*, *30*, 2931–2935.

Horton, R. E. (1940). An approach towards a physical interpretation of infiltration capacity. *Soil Science Society of America Journal*, *5*, 399–417. https://doi.org/10.2136/sssaj1941.036159950005000C0075x

Hussen, A. A., & Warrick, A. W. (1993). Algebraic models for disc tension permeameters. *Water Resources Research*, *29*(8), 2779–2786.

Iovino, M., Abou Najm, M. R., Angulo-Jaramillo, R., Bagarello, V., Castellini, M., Concialdi, P., Di Prima, S., Lassabatere, L., & Stewart, R. D. (2021). Parameterization of a comprehensive explicit model for single ring infiltration. *Journal of Hydrology*, *601*, 126801. https://doi.org/10.1016/j.jhydrol.2021.126801

Jacques, D., Mohanty, B. P., & Feyen, J. (2002). Comparison of alternative methods for deriving hydraulic properties and scaling factors from single-disc tension infiltrometer measurements. *Water Resources Research*, *38*(7), 25-1–25-14.

Lai, J., Luo, Y., & Ren, L. (2010). Buffer index effects on hydraulic conductivity measurements using numerical simulations of double-ring infiltration. *Soil Science Society of America Journal*, *74*, 1526–1536. https://doi.org/10.2136/sssaj2009.0450

Lai, J., & Ren, L. (2007). Assessing the size dependency of measured hydraulic conductivity using double-ring infiltrometers and numerical simulation. *Soil Science Society of America Journal*, *71*, 1667–1675. https://doi.org/10.2136/sssaj2006.0227

Lassabatere, L., Angulo-Jaramillo, R., Goutaland, D., Letellier, L., Gaudet, J. P., Winiarski, T., & Delolme, C. (2010). Effect of the settlement of sediments on water infiltration in two urban infiltration basins. *Geoderma*, *156*, 316–325. https://doi.org/10.1016/j.geoderma.2010.02.031

Lassabatère, L., Angulo-Jaramillo, R., Soria Ugalde, J. M., Cuenca, R., Braud, I., & Haverkamp, R. (2006). Beerkan estimation of soil transfer parameters through infiltration experiments—BEST. *Soil Science Society of America Journal*, *70*, 521–532. https://doi.org/10.2136/sssaj2005.0026

Lenhard, R. J. (1986). Changes in void distribution and volume during compaction of a forest soil. *Soil Science Society of America Journal*, *50*, 462–464. https://doi.org/10.2136/sssaj1986.03615995005000020042x

Moret-Fernández, D., Latorre, B., Lassabatere, L., Di Prima, S., Castellini, M., Yilmaz, D., & Angulo-Jaramilo, R. (2021). Sequential infiltration analysis of infiltration curves with disc infiltrometer in layered soils. *Journal of Hydrology*, *600*, 126542. https://doi.org/10.1016/j.jhydrol.2021.126542

Moret-Fernández, D., Latorre, B., López, M. V., Pueyo, Y., Lassabatere, L., Angulo-Jaramilo, R., Rahmati, M., Tormo, J., & Nicolau, J. M. (2020). Three- and four-term approximate expansions of Haverkamp formulation to estimate soil hydraulic properties from disc infiltrometer measurements. *Hydrological Processes*, *34*, 5543–5556. https://doi.org/10.1002/hyp.13966

Mualem, Y. (1976). A new model for predicting the hydraulic conductivity of unsaturated porous media. *Water Resources Research*, *12*, 513–522.

Ramos, M. C., Nacci, S., & Pla, I. (2000). Soil sealing and its influence on erosion rates for some soils in the Mediterranean area. *Soil Science*, *165*(5), 398–403.

Reynolds, W. D. (2013). An assessment of borehole infiltration analyses for measuring field-saturated hydraulic conductivity in the vadose zone. *Engineering Geology*, *159*, 119–130.

Reynolds, W. D., Drury, C. F., Tan, C. S., Fox, C. A., & Yang, X. M. (2009). Use of indicators and pore volume-function characteristics to quantify soil physical quality. *Geoderma*, *152*, 252–263.

Reynolds, W. D., & Elrick, D. E. (1990). Ponded infiltration from a single ring: I. Analysis of steady flow. *Soil Science Society of America Journal*, *54*, 1233–1241. https://doi.org/10.2136/sssaj1990.03615995005400050006x

Shan, C., & Stephens, D. B. (1995). Steady infiltration into a two-layered soil from a circular source. *Water Resources Research*, *31*(8), 1945–1952.

Šimůnek, J., Šejna, M., & van Genuchten, M. T. (2007). *The HYDRUS software package for simulating two-and three-dimensional movement of water, heat, and multiple solutes in variably-saturated media*. Technical Manual, Version 1.0. PC Progress. https://www.pc-progress.com/en/Default.aspx?h3d-downloads

Šimůnek, J., Van Genuchten, M. T., & Šejna, M. (2016). Recent developments and applications of the HYDRUS computer software packages. *Vadose Zone Journal*, *15*(7), 01–25. https://doi.org/10.2136/vzj2016.04.0033

Vandervaere, J.-P., Vauclin, M., & Elrick, D. E. (2000). Transient flow from tension infiltrometers: II. Four methods to determine sorptivity and conductivity. *Soil Science Society of America Journal*, *64*, 1272–1284. https://doi.org/10.2136/sssaj2000.6441272x

Van Genuchten, M. T. (1980). A closed-form equation for predicting the hydraulic conductivity of unsaturated soils. *Soil Science Society of America Journal*, *44*(5), 892–898. https://doi.org/10.2136/sssaj1980.03615995004400050002x

Varvaris, I., Pittaki-Chrysodonta, Z., Duus Børgesen, C., & Iversen, B. V. (2021). Parameterization of two-dimensional approaches in HYDRUS-2D. Part 1: For simulating water flow dynamics in catchment scale. *Soil Science Society of America Journal*, *85*(5), 1578–1599. https://doi.org/10.1002/saj2.20307

Wu, L., Pan, L., Roberson, M. J., & Shouse, P. J. (1997). Numerical evaluation of ring-infiltrometers under various soil conditions. *Soil Science*, *162*(11), 771–777.

Wu, L., Swan, J. B., Nieber, J. L., & Allmaras, R. R. (1993). Soil-macropore and layer influences on saturated hydraulic conductivity measured with borehole permeameters. *Soil Science Society of America Journal*, *57*, 917–923. https://doi.org/10.2136/sssaj1993.03615995005700040006x

Xu, X., Lewis, C., Liu, W., Albertson, J. D., & Kiely, G. (2012). Analysis of single-ring infiltrometer data for soil hydraulic properties estimation: Comparison of BEST and Wu methods. *Agricultural Water Management*, *107*, 34–41. https://doi.org/10.1016/j.agwat.2012.01.004

Yilmaz, D., Lassabatere, L., Angulo-Jaramillo, R., Deneele, D., & Legret, M. (2010). Hydrodynamic characterization of basic oxygen furnace slag through an adapted BEST method. *Vadose Zone Journal*, *9*, 107–116. https://doi.org/10.2136/vzj2009.0039

Yilmaz, D., Lassabatere, L., Deneele, D., Angulo-Jaramillo, R., & Legret, M. (2013). Influence of carbonation on the microstructure and hydraulic properties of a basic oxygen furnace slag. *Vadose Zone Journal*, *12*, 01–15. https://doi.org/10.2136/vzj2012.0121

How to cite this article: Bagarello, V., Iovino, M., & Lai, J. (2023). A numerical test of soil layering effects on theoretical and practical Beerkan infiltration runs. *Vadose Zone Journal*, *22,* e20283. https://doi.org/10.1002/vzj2.20283